Engineering and Technology Journal
Journal homepage: https://etj.uotechnology.edu.iq

Investigation of the Effect of SPIF Parameters on the Thickness of Al 2024 Alloy

Check for updates

Halah Ali Habeeb[a*], **Muhsin J. Jweeg**[b], **Ali Abbar Khleif**[a]

[a] Production Engineering and Metallurgy Dept., University of Technology-Iraq, Alsina'a street, 10066 Baghdad, Iraq.
[b]Al-Farahidi University, College of Technical Engineering, Aeronautical Technical Engineering Department, Baghdad - Jadriya Bridge.
*Corresponding author Email: pme.19.31@grad.uotechnology.edu.iq

HIGHLIGHTS

- The thickness thinning of Al 2024 alloy in SPIF was studied using full factorial design and ANOVA
- Effects of SPIF parameters on the thickness-thinning ratio of truncated pyramids were investigated
- Optimal parameters of 2mm thickness, 0.6 mm step depth, and 40° wall angle gave a 19.375% minimum thinning ratio

ARTICLE INFO

Handling editor: Omar Hassoon
Keywords:
SPIF process
Al 2024 sheet
Forming die
Thinning ratio
ANOVA

ABSTRACT

Sheet metal forming is one of the most commonly used manufacturing processes because millions of different parts are formed daily. In the single-point incremental forming process (SPIF), the change in the thickness of the sheet material is an essential parameter because it is an indicator of the occurrence of failure. In this context, this study investigates the effect of SPIF parameters on the thickness of the Al 2024 alloy used in producing the truncated pyramid. The process parameters were the sheet thicknesses of (1, 1.5, and 2) mm, the step depths of (0.2, 0.4, and 0.6) mm, and the wall angles of (40, 50, and 60) degrees. A full factorial design (L27) was used to design the experimental work, and a non-destructive test method was used to measure the thickness at multiple locations on the fabricated surfaces accurately. The SPIF process was performed on the CNC milling machine by the tool path (G-code) generated in the UGS-NX9 program. The data were statistically analyzed using analysis of variance (ANOVA) to determine the relationship between the SPIF parameters and the thickness changes. The results showed that the optimum value of the thinning ratio in the thickness was achieved with a thickness of 2 mm, a step depth of 0.6 mm, and a wall angle of 40°. In this regard, previous works found that a larger step size led to pronounced thickness reduction. However, this work investigated the minimum reduction in the thickness achieved at a large step size.

1. Introduction

Conventional forming processes require positive and negative dies to produce any product, which is expensive, especially when the product geometry is complex. This challenge can be eliminated or reduced using the incremental sheet metal forming processes because they do not require a complex die design, and one die can produce different geometries of the products [1, 2]. In particular, there are three types of incremental sheet metal forming processes: single-point incremental forming, double-side incremental forming, and multi-point incremental forming [3]. The most commonly used process is the single-point incremental forming process. This process requires the tool and the forming die, which usually consists of many parts, such as a blank holder, a backing plate, screws, and nuts [4]. The single-point incremental forming process uses computer numerical control (CNC) machines, where the tool is fixed instead of the cutting tool that moves in the z-direction. In contrast, the forming die is fixed on the machine table that moves in the x and y directions [5]. To form the required product geometry, the tool moves along a specific path using the CNC milling machine or the robots, and the forming process is carried out layer by layer, as shown in Figure 1 [6, 7].

http://doi.org/10.30684/etj.2023.143718.1604
Received 1 November 2023; Received in revised form 25 November 2023; Accepted 28 November 2023; Available online 15 December 2023
2412-0758/University of Technology-Iraq, Baghdad, Iraq
This is an open access article under the CC BY 4.0 license http://creativecommons.org/licenses/by/4.0

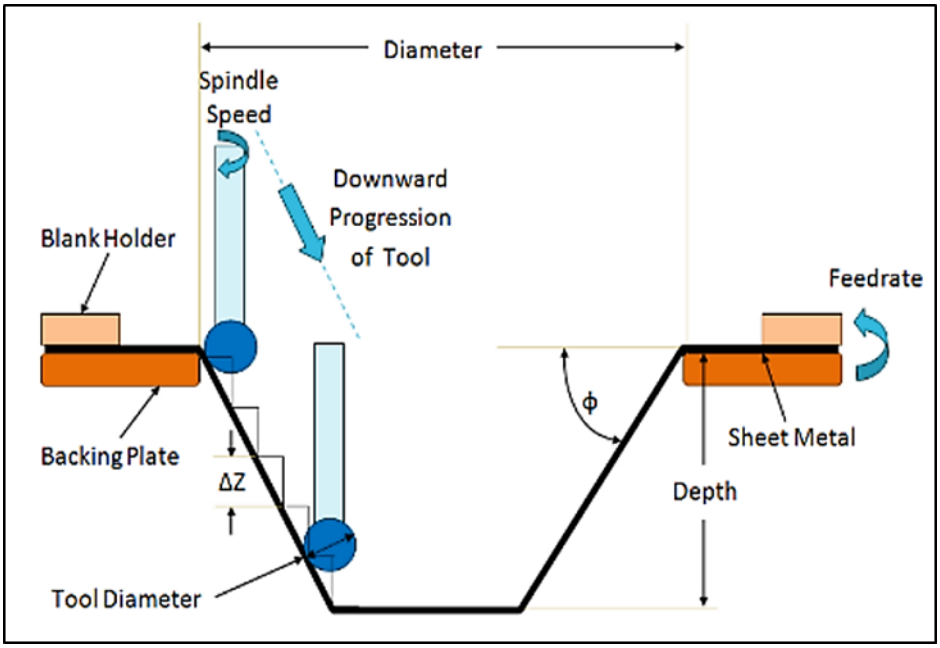

Figure 1: The SPIF process [8]

One of the challenges in the single-point incremental forming process is the thinning ratio in the thickness, which is directly related to the material's formability. Therefore, many researchers have studied the effect of the SPIF process parameters on the thickness's thinning ratio [9].

For instance, Popp et al. [10] studied force generation and wall thinning during the formation of the cranial implant using the single-point incremental forming process. Particularly, the sheet metal used was (S700) with a thickness of (4 mm). The finite element analysis (Abaqus) program was used to simulate the cranial implant's single-point incremental forming process and find the material's force and thickness reduction. The results showed that the maximum predication force is (25.9 KN) and the maximum predication thickness reduction is (46 %). In another work, Rosca et al. [11] conducted a numerical-experimental study of the single-point incremental forming process. The sheet metal is steel (DC04) with a thickness of 0.6 mm, and the geometry produced is a truncated cone. The Ls-Dyna simulated the single-point incremental forming process and measured the major minor strains, thickness distribution, and forces. The results from the numerical analysis agreed well with those from the experimental work. Moreover, Zhu et al. [12] presented the forming tool path generated using the stretching angle in the multi-incremental forming process. The material used is aluminum alloy (Al 1060) with a thickness of 1 mm, and the tool path was generated using C++, VC++, and the OpenGL library. In addition, the ANSYS/LS-DYNA was used as a finite element analysis to simulate the sheet's strain and thickness distribution. The results confirmed that stretching angle 15 gave high dimensional accuracy and a larger thickness of the formed product than stretching angle 5. Furthermore, Murugesan and Jung [13] studied the effect of forming process parameters in the single-point incremental forming process on the formability and failure evaluation. The material used is an aluminum alloy (AA 3003-H18) with a thickness of 0.5 mm, and the geometries produced were a truncated cone and a truncated pyramid. The design of the experiment, the grey relation analysis, and the analysis of variance were applied to enhance the formability without failure. The response surface methodology was used to design the experimental works, and the input parameters were the step size, the tool radius, and the feed rate. The microstructural inspection showed that the thinning increases when it reaches the maximum forming depth. Ullah et al. [14] presented various methodologies to improve the geometric accuracy of products formed using the double-sided incremental forming process. More specifically, the methodologies studied the sheet thickness variation, the fracture mechanism, the tool force, and the support tool's role in double-sided incremental forming. The results showed that the triple-point incremental forming gives good geometric accuracy compared with the single and double-sided point incremental forming, and the spring-back can be reduced when using the double-sided incremental forming. Additionally, Mohammed et al. [15] presented the influence of the anisotropy in the single-point incremental forming process of aluminum bilayer sheets (Al 20 and Al 70). In particular, the finite element method (Abaqus) was used to investigate the effect of layer arrangement and the anisotropy of sheet metal according to the rolling direction on the thickness, the forming reaction force, and the plastic strain. Moreover, the comparison between isotropic and anisotropic was conducted. The MATLAB program was used to generate the tool path of the truncated cone. The results showed that the formability was better with the Al-70 / Al-20-layer arrangement. However, it gave a higher reaction force.

This work aims to study the effect of the SPIF process parameters on the thickness ratio and use ANOVA to investigate the optimum value of the thickness ratio. In fact, this work aligns with the literature review investigating the effect of the SPIF parameters on the thickness change. Still, it studied the thickness change of the Al 2024 alloy, while the other works presented the thickness change for various materials.

2. Material and Geometry of the Product

The sheet material used was aluminum alloy (Al 2024), and the chemical composition of this alloy is listed in Table 1. The product's geometry produced by the SPIF process was a truncated pyramid with a total depth in the z-direction of 30 mm, as shown in Figure 2 (a, b, and c). The SolidWorks package was used to design the product geometry, and the UGS-NX9 was used to generate the G-code (the tool path) that was transferred to the CNC milling machine to perform the SPIF process. In this regard, pyramid geometries are used in many industrial applications, such as material handling and conveyor systems, aerospace and defense (sensor housings, antennae, and aerodynamic structures), and storage containers.

Table 1: The Al 2024 chemical compositions

Element	Si	Fe	Cu	Mn	Mg	Cr	Zn	Ti	V	Zr	Other	Al
Weight %	0.07	0.18	4.6	0.6	1.3	0.01	0.09	0.02	0.01	0	0.03	Remainder

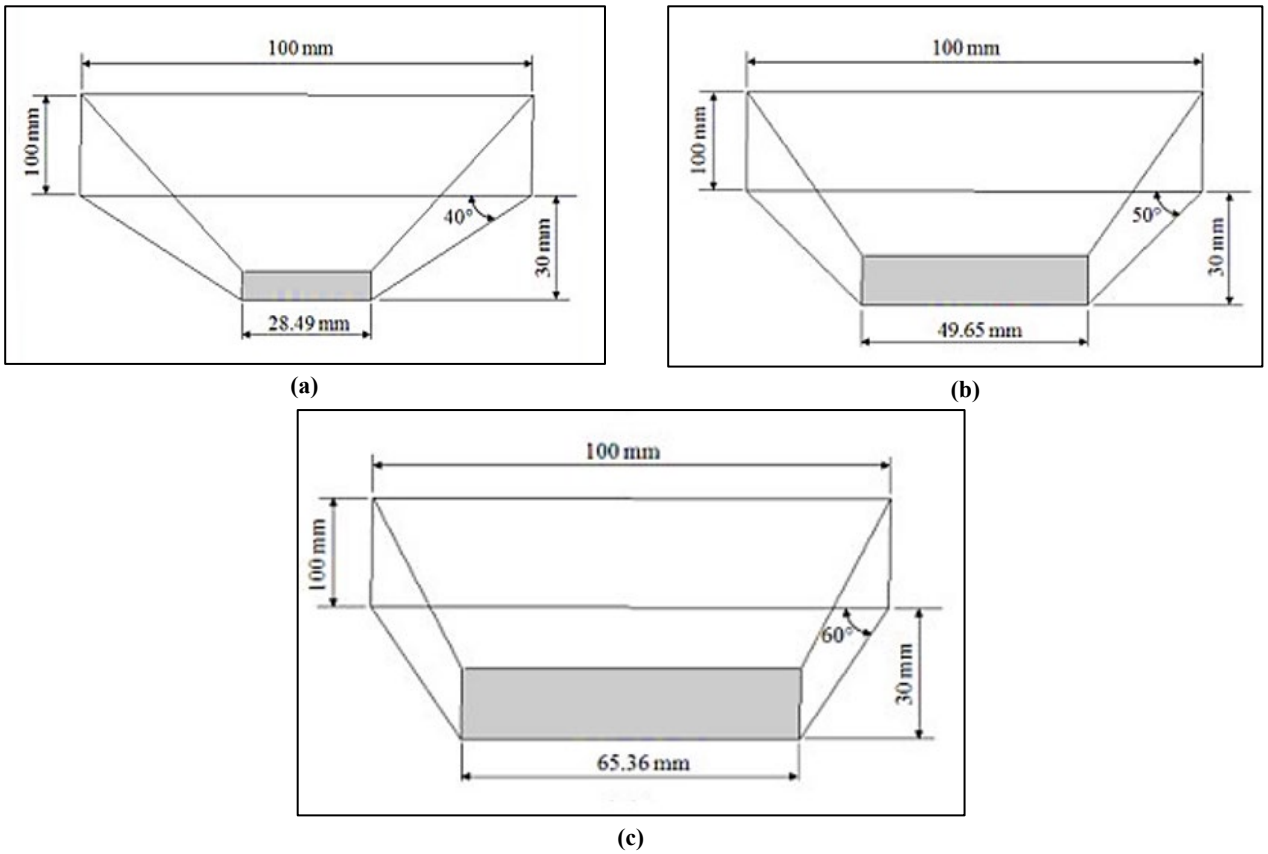

Figure 2: The geometry of the truncated pyramid (a) a wall angle of 40º, (b) a wall angle of 50º, and (c) a wall angle of 60º

3. Theoretical Considerations

The measurement of the product walls' thickness is presented in this work. In particular, the sine law equation is used for measuring the thickness of the products formed by the single-point incremental forming process. The sine law assumes that the volume and the deformation with the plane strain remain constant. More precisely, Equation 1 is used to measure the final thickness, and this equation gives accurate measurements only for the flat surface produced by the SPIF process [3].

$$t_f = t_o \sin\left(\frac{\pi}{2} - \alpha\right) \quad (1)$$

where: t_f: The thickness after forming. t_o: The original thickness of the sheet. α : The wall angle.

However, if the surfaces are non-flat, the thickness after deformation can be calculated easily as a function of the area ratio of the undeformed and the deformed sheet metals, as illustrated in Equation 2:

$$t_f = t_o \cdot \frac{A_o}{A_f} \quad (2)$$

where: A_o: The original area of the sheet. A_f: The area of the sheet after deformation.

In the SPIF process, the deformation process is a nonlinear large displacement. The continuous squeezing of the metal while the tool is moving leads to plastic deformation. Moreover, the greater force in the SPIF process is axial greater than tangential and radial forces. Therefore, the shear deformation is usually assumed to occur in the axial direction, as shown in Figure 3 [9].

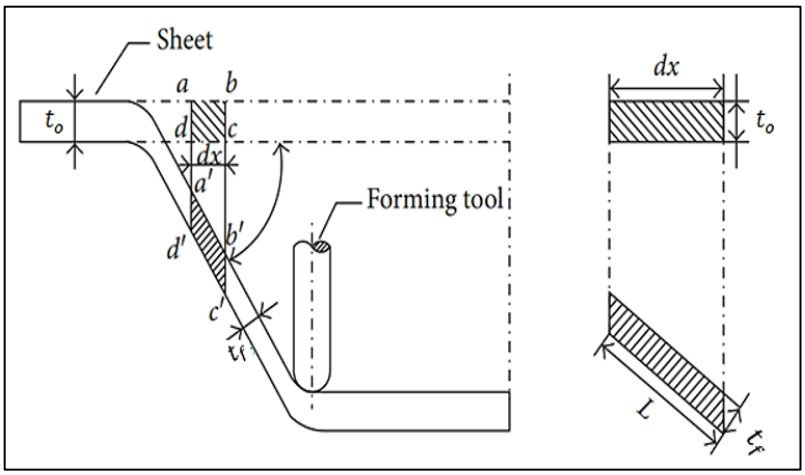

Figure 3: Shear deformation in the SPIF process [9]

Based on the constant volume in plastic deformation, Equation 3 can be obtained:

$$d_x\, t_o = L\, t_f \quad \Rightarrow \quad d_x = L \cos\alpha \tag{3}$$

The wall thinning rate provides a sense of the change in the metal thickness and is an important formability parameter. To this end, lower strength and accuracy of the produced product will result when the rate of wall thickness reduction falls within certain limits. In this context, Equation 4 can be used to determine the rate of the wall thickness thinning:

$$\varphi = \frac{t_o - t_f}{t_o} \times 100\ \% \tag{4}$$

where: φ : The thinning rate in the thickness.

4. Experimental Work

In this work, the SPIF process was carried out using the CNC milling machine and the forming die, as shown in Figure 4, which is fixed on the machines' table, and the tool's geometry used was hemispherical with a diameter of 8 mm. The forming die parts (the clamping plate, the backing plate, the top plate, and the base plate) were manufactured using the CNC Oxy-Plasma cutting machine, and the finishing dimensions for these parts were achieved using the CNC milling machine.

The SPIF process parameters were the wall angle, the thickness, and the step depth, as illustrated in Table 2. The design of experiment tests was done using the full factorial design (L27) method in the Mini Tab program, as listed in Table 3.

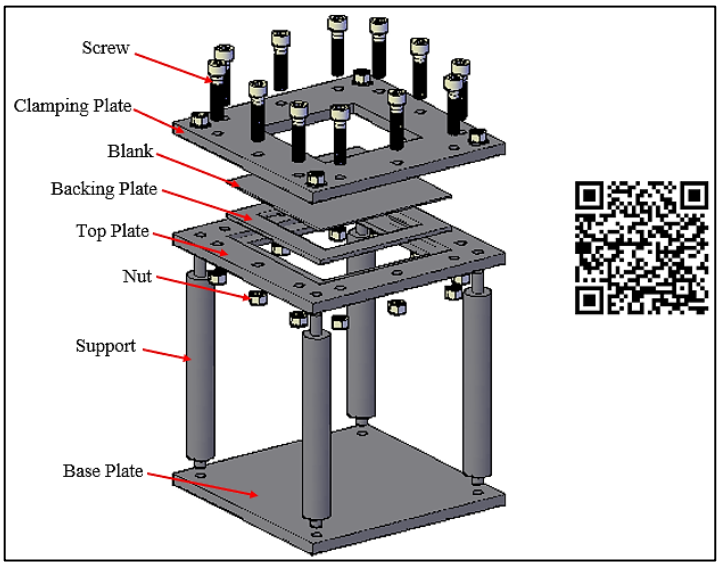

Figure 4: The forming frame parts used in the SPIF process

Table 2: The SPIF process parameters and their levels

Parameter	Units	Level 1	Level 2	Level 3
Wall angle	degree	40	50	60
Thickness	mm	1	1.5	2
Step depth	mm	0.2	0.4	0.6

Table 3: The experimental design of the SPIF process

Experiment No.	Process Parameters		
	Wall angle (°)	Thickness (mm)	Step depth (mm)
1	60	2	0.6
2	40	1	0.4
3	40	2	0.2
4	40	1.5	0.4
5	60	1.5	0.2
6	60	2	0.4
7	40	1	0.2
8	60	1	0.6
9	60	1.5	0.4
10	50	1.5	0.4
11	40	1	0.6
12	40	1.5	0.6
13	60	1	0.2
14	60	1	0.4
15	50	1.5	0.6
16	50	1	0.4
17	60	2	0.2
18	60	1.5	0.6
19	50	2	0.4
20	40	2	0.4
21	50	2	0.6
22	50	1	0.6
23	50	1	0.2
24	50	2	0.2
25	40	2	0.6
26	40	1.5	0.2
27	50	1.5	0.2

The SPIF process was performed on the CNC milling machine, as shown in Figure 5, and the products are shown in Figure 6. The other parameters of the process were constant, including a feed rate of 800 mm/min [16], zero spindle speed, a hemispherical end tool with a diameter of 8 mm [17], and the lubricant used was SAE 5W-30.

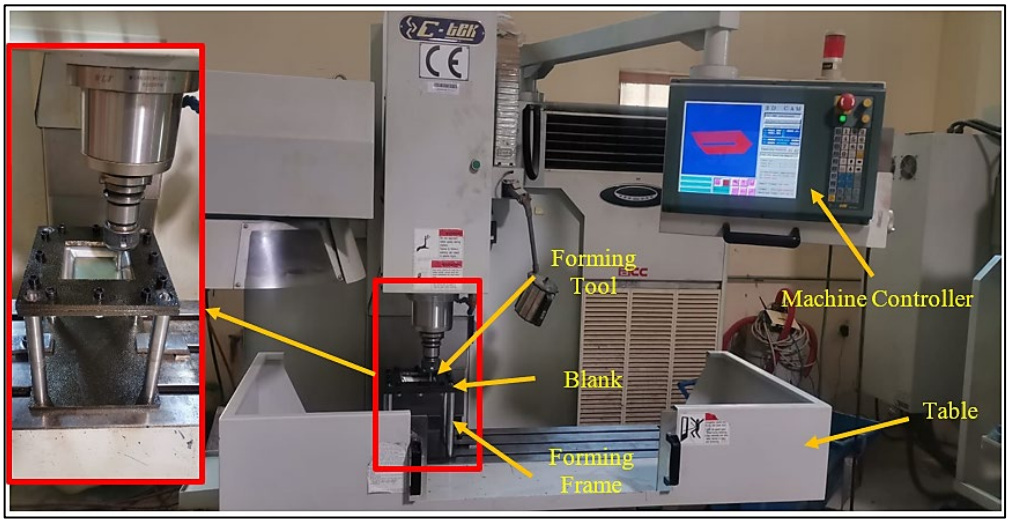

Figure 5: The CNC milling machine used in the SPIF process

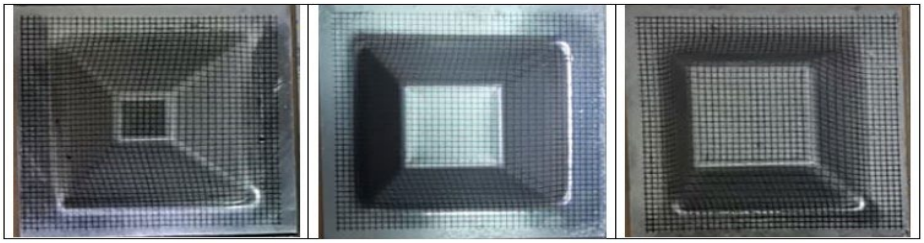

Figure 6: The products produced using the SPIF process

5. Thickness Measurement

In the single-point incremental forming process, the change in the thickness of the sheet material is an essential parameter because it is an indicator of the occurrence of the failure. The measurement process takes place along two lines, each of which consists of three regions that start from the center of the base of the pyramid product to the flange of the product, as shown in Figure 7, one of which is at a zero angle and the other is at a 45° angle. The thinning ratio is obtained based on Equation 4, and the thickness of the wall is measured in four positions for every region using the digital dial gauge indicator, as shown in Figure 8. The measuring range of this gauge is (0-12.7 mm), and the resolution is (0.001 mm).

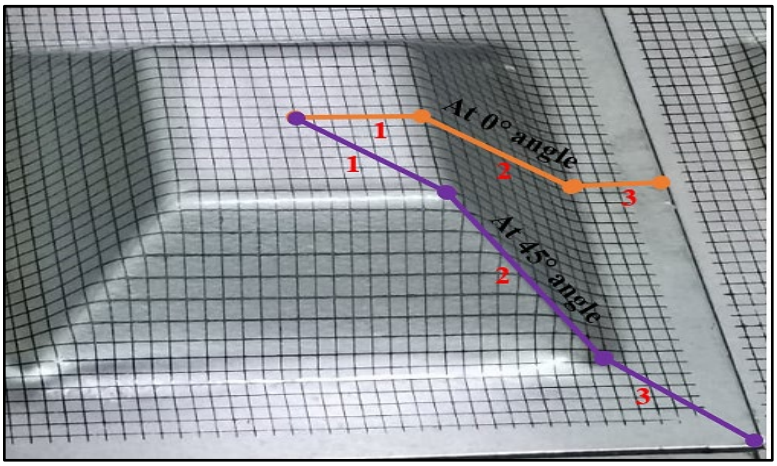

Figure 7: The measured regions

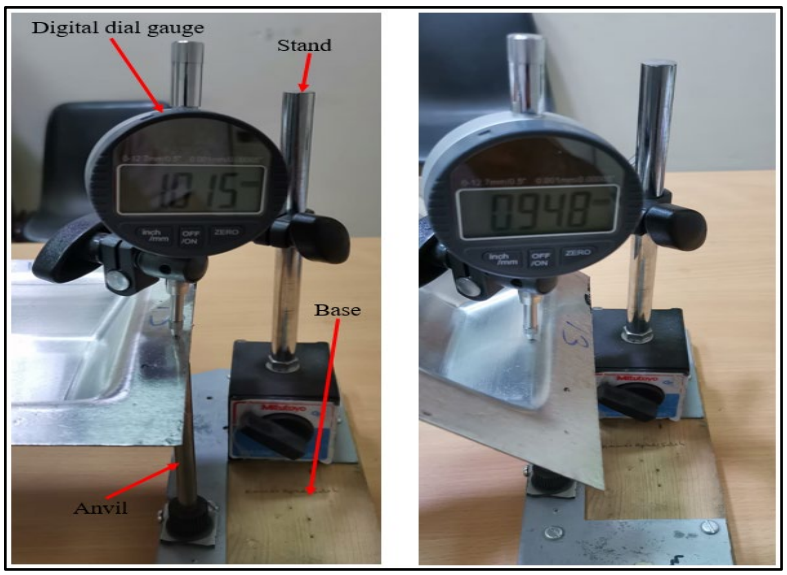

Figure 8: The measuring method of the thickness

6. Results and Discussion

The change in thickness in the second zone will be studied to observe the noticeable change in this zone compared to those in the first and the third zones, where the change in thickness is not noticeable and is very slight. In particular, four thickness measures were taken in the second region, and the average was calculated, as listed in Table 4.

Table 4: The thickness after forming

Experiment No.	Region 2 (From the base of the product to the top of the flange)									
	At an angle of 0°					At an angle of 45°				
	Value 1	Value 2	Value 3	Value 4	Average	Value 1	Value 2	Value 3	Value 4	Average
1	1.3	1.3	1.7	2.1	1.6	1.1	1.1	1.4	1.9	1.375
2	0.7	0.75	0.8	1.1	0.8375	0.7	0.7	0.75	0.8	0.7375
3	1.5	1.55	1.6	2.1	1.6875	1.4	1.45	1.65	1.82	1.58
4	1.15	1.15	1.2	1.6	1.275	1.1	1.05	1.05	1.2	1.1
5	0.8	0.95	1	1.6	1.0875	0.65	0.7	0.8	1.3	0.8625
6	1.2	1.3	1.35	2.05	1.475	0.95	1.05	1.3	1.9	1.3
7	0.8	0.85	0.9	1.1	0.9125	0.7	0.75	0.8	0.9	0.7875
8	0.8	0.75	0.75	1.1	0.85	0.5	0.55	0.6	0.9	0.6375
9	0.85	0.95	1	1.65	1.1125	0.75	0.75	0.75	1.4	0.9125
10	0.95	1.05	1.1	1.6	1.175	0.85	0.85	0.9	1.65	1.0625
11	0.7	0.75	0.8	1.05	0.825	0.7	0.7	0.75	0.95	0.775
12	1.2	1.3	1.3	1.75	1.3875	1.1	1.1	1.1	1.3	1.15
13	0.7	0.75	0.75	1.15	0.8375	0.55	0.65	0.8	1.1	0.775
14	0.7	0.75	0.75	1.15	0.8375	0.55	0.65	0.7	0.95	0.7125
15	1	1.15	1.2	1.7	1.2625	0.9	0.9	0.95	1.4	1.0375
16	0.7	0.8	0.85	1.1	0.8625	0.6	0.7	0.75	0.9	0.7375
17	1.2	1.3	1.5	2.2	1.55	0.95	1.05	1	1.85	1.2125
18	1	1.05	1.1	1.2	1.0875	0.75	0.85	1	1.35	0.9875
19	1.3	1.4	1.5	2.2	1.6	1.15	1.15	1.25	1.45	1.25
20	1.5	1.6	1.65	2.1	1.7125	1.4	1.4	1.45	1.85	1.525
21	1.2	1.35	1.5	2.2	1.5625	1.1	1.15	1.25	1.7	1.3
22	0.65	0.7	0.8	1.1	0.8125	0.6	0.65	0.7	0.85	0.7
23	0.6	0.65	0.7	1.05	0.75	0.6	0.65	0.7	0.8	0.6875
24	1.3	1.35	1.5	2.1	1.5625	1.1	1.2	1.25	1.55	1.275
25	1.55	1.6	1.7	2.05	1.725	1.45	1.55	1.65	1.8	1.6125
26	1.1	1.15	1.2	1.7	1.2875	1.05	1.05	1.1	1.35	1.1375
27	0.95	1	1.15	1.7	1.2	0.8	0.85	0.85	1.25	0.9375

To obtain a clearer impression regarding the change in the thickness of the sheet material, the wall thinning ratio was obtained using Equation 4, and the results are listed in Table 5. Moreover, Figure 9 shows the wall thinning ratio of the truncated pyramid products due to the single-point incremental forming process in the second region and along the line inclined at zero angles and the line inclined at 45 degrees.

Table 5: The wall thinning ratio

Experiment No.	t_o (mm)	At an angle of 0°		At an angle of 45°	
		t_f (mm)	φ %	t_f (mm)	φ %
1	2	1.6	20	1.375	31.25
2	1	0.8375	16.25	0.7375	26.25
3	2	1.6875	15.625	1.58	21
4	1.5	1.275	15	1.1	26.667
5	1.5	1.0875	27.5	0.8625	42.5
6	2	1.475	26.25	1.3	35
7	1	0.9125	8.75	0.7875	21.25
8	1	0.85	15	0.6375	36.25
9	1.5	1.1125	25.833	0.9125	39.167
10	1.5	1.175	21.667	1.0625	29.167
11	1	0.825	17.5	0.775	22.5
12	1.5	1.3875	7.5	1.15	23.333
13	1	0.8375	16.25	0.775	22.5
14	1	0.8375	16.25	0.7125	28.75
15	1.5	1.2625	15.833	1.0375	30.833
16	1	0.8625	13.75	0.7375	26.25
17	2	1.55	22.5	1.2125	39.375
18	1.5	1.0875	27.5	0.9875	34.167
19	2	1.6	20	1.25	37.5
20	2	1.7125	14.375	1.525	23.75
21	2	1.5625	21.875	1.3	35
22	1	0.8125	18.75	0.7	30
23	1	0.75	25	0.6875	31.25
24	2	1.5625	21.875	1.275	36.25
25	2	1.725	13.75	1.6125	19.375
26	1.5	1.2875	14.167	1.1375	24.167
27	1.5	1.2	20	0.9375	37.5

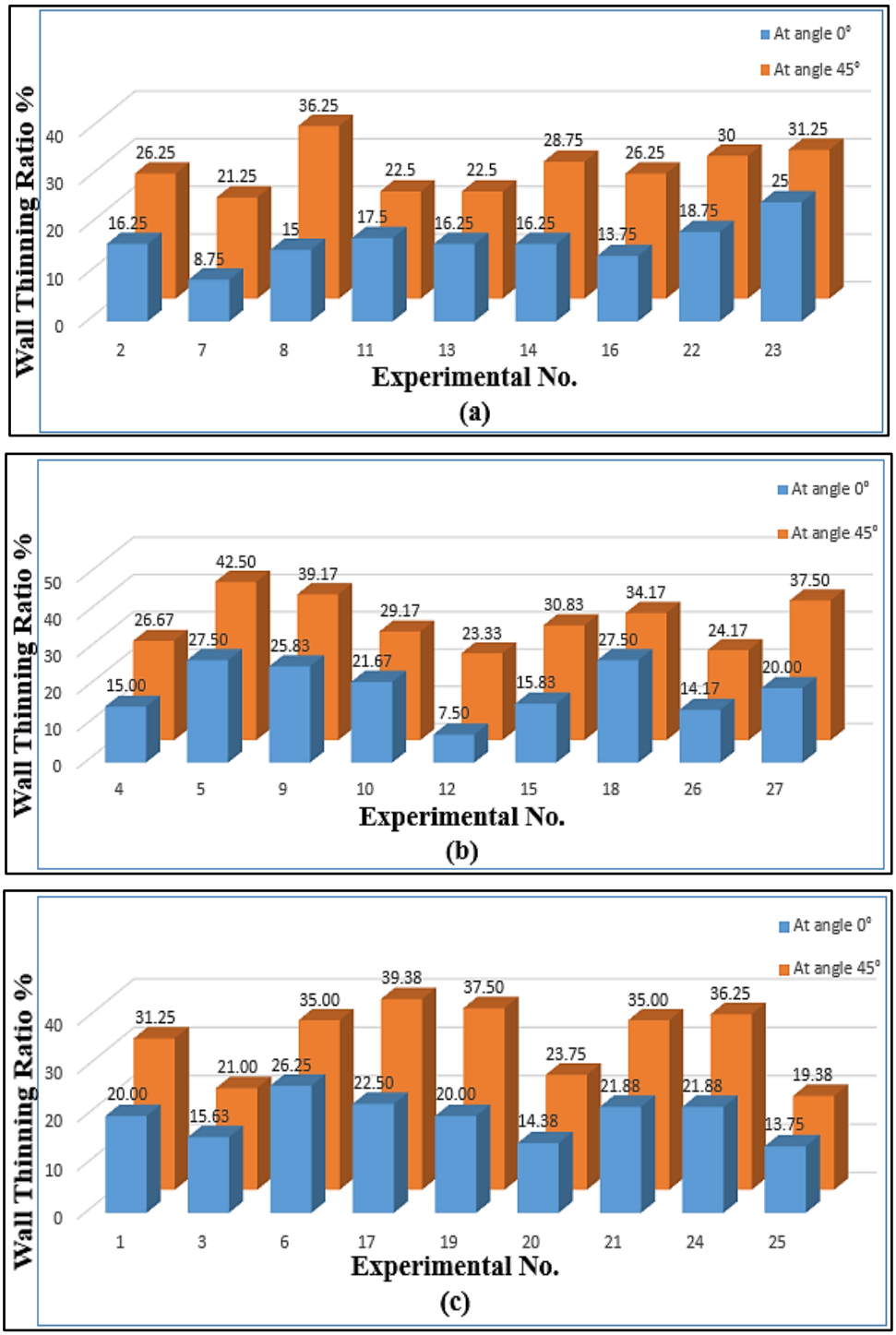

Figure 9: The wall thinning ratio with different thicknesses (a) 1 mm, (b) 1.5 mm, and (c) 2 mm

From Figure 9 (a, b, and c), we notice that the wall thinning ratio at the line inclined at 45 degrees is the highest compared with the wall thinning ratio at the line along the zero angle. Therefore, the line results with an angle of 45 degrees will be adopted as the output in the experiment design (full factorial design). The Mini Tab program with full factorial design calculates the relationship between the wall thinning ratio and the process parameters (the wall angle, the thickness, and the step depth). Figure 10 (a, b, and c) presents the relationship among the results extracted from the experimental work.

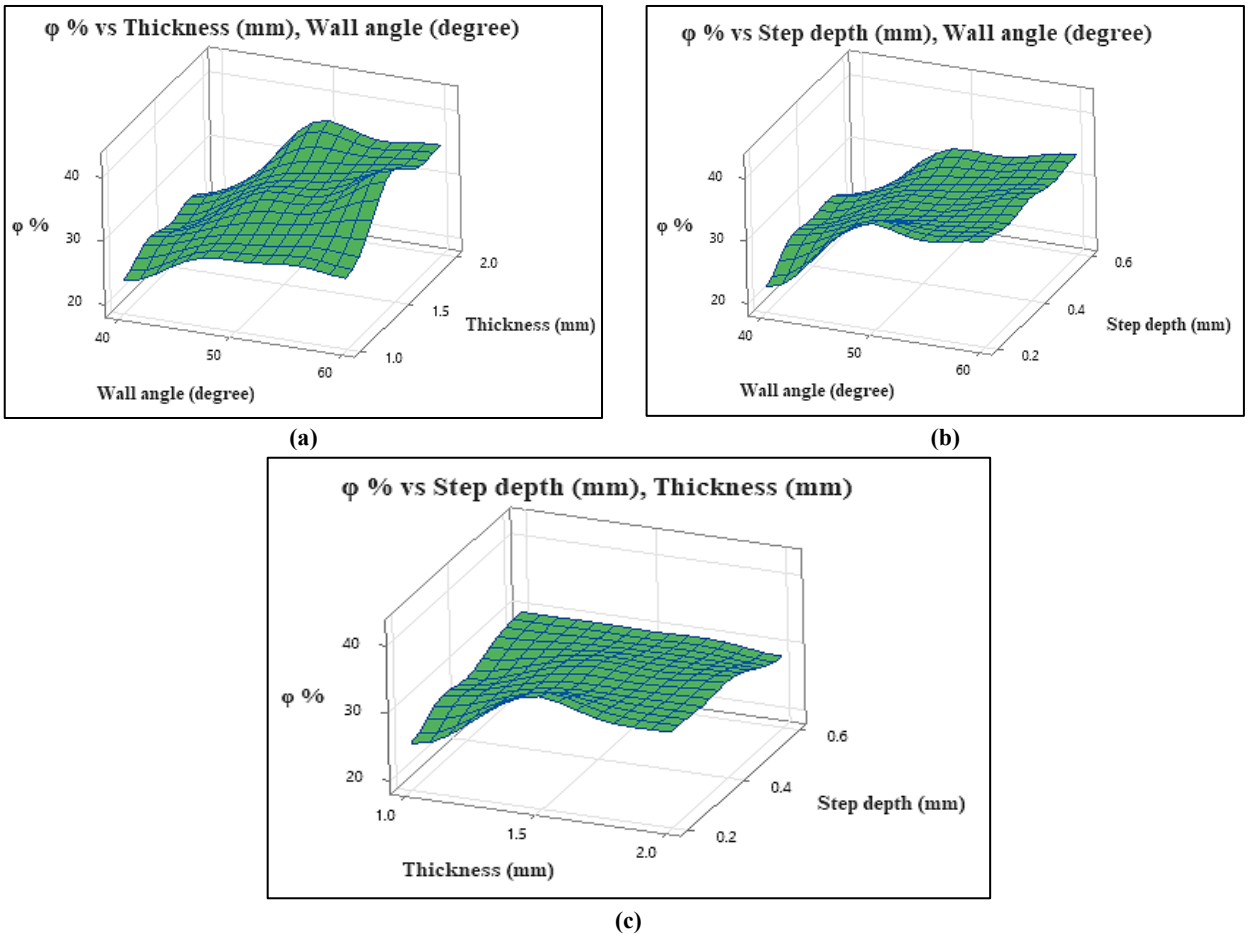

Figure 10: The relationship between the wall thinning ratio and the process parameters

Figure 11 shows the Pareto chart, which is used to identify the effect of the process parameters on the outputs (the wall thinning ratio). In this regard, the wall angle parameter greatly affects the wall thinning ratio, followed by the thickness of the sheet material and then the step depth. Furthermore, the analysis of variance (ANOVA) was used to show the relationship between the process parameters and the mean response (the wall thinning ratio), as demonstrated in Figure 12. In this work, linear regression was used to model the single-point incremental forming process parameters to obtain the wall-thinning ratio:

$$\varphi\ \% = -2.06 + 0.559 * Wall\ angle\ (deg) + 3.72 * Thickness\ (mm) - 3.63 * Step\ depth\ (mm) \quad (5)$$

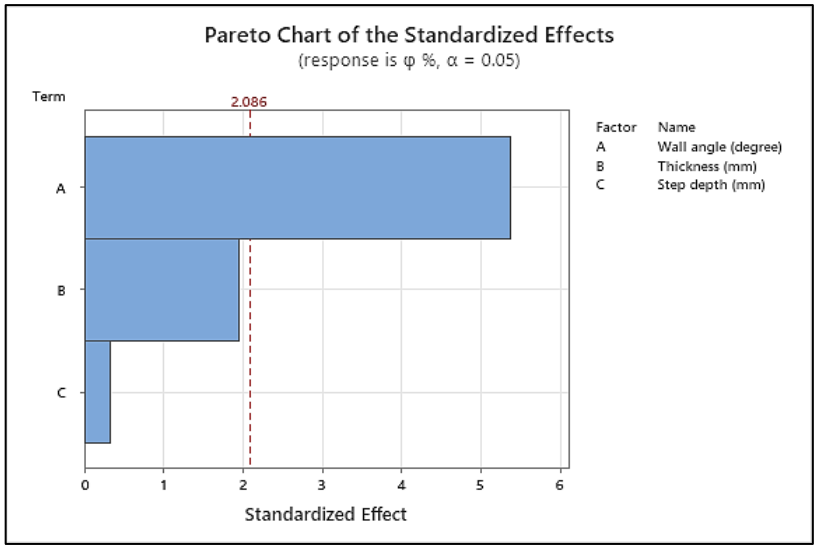

Figure 11: The Pareto chart for the effect of the SPIF process parameters on φ

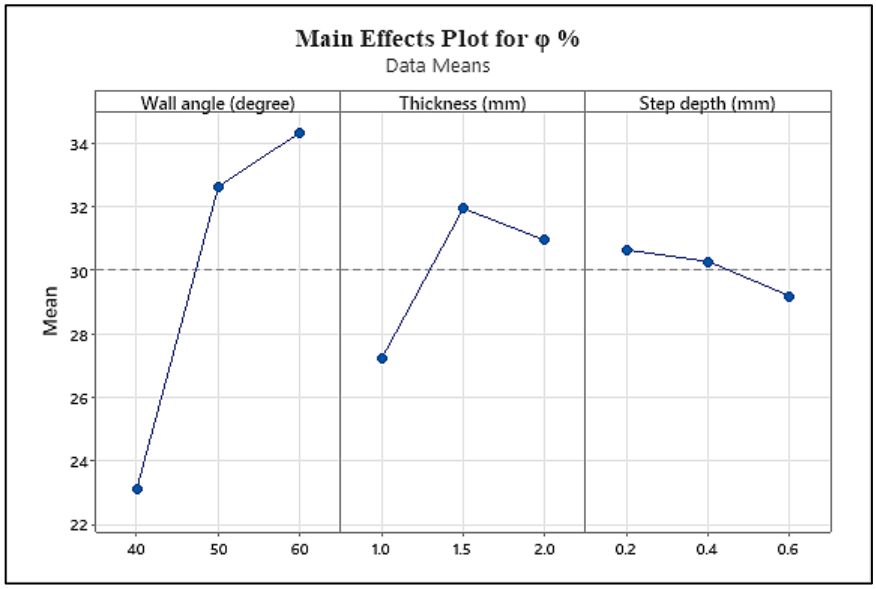

Figure 12: The relationship between the process parameters and the mean (φ)

The results indicate that the wall thinning ratio is directly proportional to the wall angle of the truncated pyramid and is inversely proportional to the step depth. Moreover, the relationship between the wall thinning ratio and the sheet thickness changes with the change in thickness. More specifically, when the sheet thickness is (1 mm), the wall thinning ratio is at its lowest value, and when the sheet thickness increases to (1.5 mm), we notice an increase in the value of the wall thinning ratio. However, at further increases in thickness to (2 mm), the value of the wall thinning ratio decreased.

The increase in the wall angle led to an increase in the wall thinning ratio because the thickness after forming decreases according to Equation 1. In addition, increasing the step depth leads to a decrease in the wall-thinning ratio due to the minimum contact points between the tool and the sheet material, which leads to a slight change in the thickness compared to the small step depth.

Particularly, the lowest value of the wall thinning ratio was obtained when the wall angle was (40°), the sheet thickness was (2 mm), and the step depth was (0.6 mm). In contrast, the highest value of the wall thinning ratio was obtained when the wall angle was (60°), the sheet thickness was (1.5 mm), and the step depth was (0.2 mm).

7. Conclusion

Based on the results that were obtained and analyzed, the main conclusions of this work can be summarized:

1) From the full factorial design (L27) and the ANOVA results, the optimum level for the minimum wall thinning ratio (φ) parameter was obtained at the third level of the step depth, the sheet thickness, and the first level of the wall angle.
2) The wall thinning ratio (φ) increased as the wall angle increased because the thickness decreased at a high value of the wall angle, leading to an increase in the wall thinning ratio. On the other hand, it decreased when increasing the step depth due to a decrease in contact points between the tool and the sheet material, which led to a slight change in the thickness.
3) The wall thinning ratio (φ) increased with the sheet thickness. But when the sheet thickness has a value greater than 1.5 mm, the wall thinning ratio (φ) was decreased.
4) Increasing the thinning in thickness leads to increasing the thickness strain, which leads to failure at a high value of wall thinning.
5) The wall thinning ratio at the corners of the truncated pyramid has a larger value than at other wall regions because, at corners, the material was subjected to stretching and bending, while in other regions subjected to stretching.
6) Finally, the research contributes to optimizing the thickness control of the Al 2024 alloy in the SPIF process. Consequently, it enables the manufacturers to achieve precise thickness profiles.

Author contributions

Conceptualization, H. Habeeb, M. Jweeg and A. Khleif; writing—original draft preparation, H. Habeeb, M. Jweeg and A. Khleif; writing—review and editing, H. Habeeb, M. Jweeg and A. Khleif; supervision, M. Jweeg and A. Khleif. All authors have read and agreed to the published version of the manuscript.

Funding

This research received no specific grant from any funding agency in the public, commercial, or not-for-profit sectors.

Data availability statement

The data that support the findings of this study are available on request from the corresponding author.

Conflicts of interest

The authors declare that there is no conflict of interest.

References

[1] N. H. Obaeed, Numerical and Experimental Explorations for the Formability of Drawing Square Cups Through Deep Drawing Operation, Eng. Technol. J., 38 (2020) 1316-1326. https://doi.org/10.30684/etj.v38i9A.1340

[2] B. A. Ahmed, S. K. Shather, and W. K. Hamdan, Improve the Micro-hardness of Single Point Incremental Forming Product Using Magnetic Abrasive Finishing, Eng. Technol. J., 38 (2020) 1137-1142. http://dx.doi.org/10.30684/etj.v38i8A.906

[3] R. Esmaeilpour, H. Kim, T. Park, F. Pourboghrat, A. Agha, and F. Abu-Farha, Effect of hardening law and process parameters on finite element simulation of single point incremental forming (SPIF) of 7075 aluminum alloy sheet, Mechanics & Industry, 21(2020). https://doi.org/10.1051/meca/2020019

[4] K. Zaba, S. Puchlerska, Ł. Kuczek, T. Trzepieci´nski, and P. Maj, Effect of Step Size on the Formability of Al/Cu Bimetallic Sheets in Single Point Incremental Sheet Forming, Materials, 16 (2023). https://doi.org/10.3390/ma16010367

[5] Abdul Qadeer, G. Hussain, Mohammed Alkahtani, and Johannes Buhl, Springback behavior of a metal/polymer laminate in incremental sheet forming: stress/strain relaxation perspective, J. Mater. Res. Technol., 23 (2023) 1725-1737. https://doi.org/10.1016/j.jmrt.2023.01.088

[6] Abdul Qadeer, G. Hussain, Mohammed Alkahtani, and Johannes Buhl, Springback behavior of a metal/polymer laminate in incremental sheet forming: stress/strain relaxation perspective, J. Mater. Res. Technol., 23 (2023) 1725-1737. https://doi.org/10.1016/j.jmrt.2023.01.088

[7] S. Thiery, M. Zein El Abdine, J. Heger, and N. Ben Khalifa, Closed-loop control of product geometry by using an artificial neural network in incremental sheet forming with active medium", Int. J. Mater. Forming, 14 (2021) 1319–1335. https://doi.org/10.1007/s12289-020-01598-1

[8] A. S. Baden, Optimization and prediction of process parameters in SPIF that Affecting on surface quality using simulated annealing algorithm, Al-Khwarizmi Eng. J., 12 (2016) 81-92. http://dx.doi.org/10.22153/kej.2016.05.005

[9] M. Yang, ZimengYao, Yan Li, Pengyang Li, Fengkui Cui, and Lang Bai, Study on Thickness Thinning Ratio of the Forming Parts in Single Point Incremental Forming Process, Adv. Mater. Sci. Eng., 2018 (2018) 1-11. https://doi.org/10.1155/2018/2927189

[10] M. Popp, G. Rusu, S. Racz, and I. Octavian Popp, Force and thickness prediction with FEA of the cranial implants manufactured through SPIF, MATEC Web of Conferences 290 (2019). http://dx.doi.org/10.1051/matecconf/201929004008

[11] N. Rosca, M. Oleksik, and L. Rosca, Numerical-Experimental Study Regarding the Single Point Incremental Forming Process, MATEC Web of Conferences, 343 (2021). https://doi.org/10.1051/matecconf/202134303008

[12] H. Zhu, G. Cheng, and D. Jung, Toolpath Planning and Generation for Multi-Stage Incremental Forming Based on Stretching Angle, Materials, 14 (2021) 4828. https://doi.org/10.3390/ma14174818

[13] M. Murugesan and D. Won Jung, Formability and Failure Evaluation of AA3003-H18 Sheets in Single-Point Incremental Forming Process through the Design of Experiments, Mater., 14 (2021) 808. https://doi.org/10.3390/ma14040808

[14] S. Ullah, P. Xu, X. Li, Y. Li, K. Han, and D. Li, A Review on Part Geometric Precision Improvement Strategies in Double-Sided Incremental Forming, Metals, 12 (2022) 103. https://doi.org/10.3390/met12010103

[15] B. Abdullah Mohammed, R. Sabri Batbooti, and T. Ali Jabbar, Numerical study on the effect of anisotropy on deformation behavior of aluminum bilayer sheets in single point incremental metal forming, East. -Eur. J. Enterp. Technol., 3 (2022) 50-57. https://doi.org/10.15587/1729-4061.2022.256225

[16] M. M. Abdulrazaq, S. K. Gazi, and M. Q. Ibraheem, Investigation the Influence of SPIF Parameters on Residual Stresses for Angular Surfaces Based on Iso-Planar Tool Path, Al-Khwarizmi Eng. J., 15 (2019) 50-59. https://doi.org/10.22153/kej.2019.09.002

[17] Harshavardhana Natarajan, Sundar Singh Sivam Sundarlingam Paramasivam, Durai Kumaran, G. Sai Krishnan, Shajahan Shariq Ibrahim, Application of MABAC in support of decision-making on the key process variables in sheet metal forming, Mater. Today: Proc., 47 (2021)7140-7144 . https://doi.org/10.1016/j.matpr.2021.06.309